Dynamics of a generalized fashion cycle model

Iryna Sushko[a], Laura Gardini[b], Kiminori Matsuyama[c]
[a]Institute of Mathematics, NASU, and Kyiv School of Economics, Ukraine
[b]Dept of Economics, Society and Politics, University of Urbino, Italy
[c]Dept of Economics, Northwestern University, USA

Abstract

We study a four-parameter family of 2D piecewise linear maps with two discontinuity lines. This family is a generalization of the discrete-time version of the fashion cycle model by Matsuyama, which was originally formulated in continuous time. The parameter space of the considered map is characterised by quite a complicated bifurcation structure formed by the periodicity regions of various attracting cycles. Besides the standard period adding and period incrementing structures, there exist incrementing structures with some distinctive properties, as well as novel mixed structures, which we study in detail. The boundaries of many periodicity regions associated with border collision bifurcations of the related cycles are obtained analytically. Several mixed structures are qualitatively described.

Keywords: Fashion cycle model, 2D discontinuous piecewise linear map, Border collision bifurcation, Period adding bifurcation structure, Period incrementing bifurcation structure.

1 Introduction

In [12] Matsuyama proposes the *continuous-time* fashion cycle model, a game played by Conformists, who want to act or look the same with others, and by Nonconformists, who want to act or look different from others. It is shown in [12] that the dynamical system associated with this game is characterized by discontinuous piecewise linear functions, and, depending on the parameters, has either attracting fixed points, which he interprets as *the social custom*, or a unique limit cycle, which he interprets as *the fashion cycle*.

In [7] we reformulate this model in a *discrete-time* setting leading to a *2D discontinuous piecewise linear map* $G : I^2 \to I^2$, $I^2 = [0,1] \times [0,1]$, and show that besides the attracting fixed points this map can have attracting cycles of different periods, possibly coexisting. In addition to the period adding and period incrementing bifurcation structures[1], we show the existence of several partially overlapping incrementing structures in the parameter space of map G. Furthermore, we prove that if the time-delay in the discrete time model tends to zero, the number of period incrementing structures tends to infinity and the dynamics of the discrete time fashion cycle model converges to those of the continuous-time fashion cycle model.

One of the characteristic properties of map G is its symmetry with respect to the center of the unit square, moreover, this map is defined by four 2D linear maps with uncoupled variables in four different subregions of I^2, where each linear map is a contraction with *equal* real eigenvalues. The period adding and period incrementing bifurcation structures, mentioned above, are associated with attracting cycles having rather simple symbolic sequences. This helps to obtain in explicit form all the boundaries of the existence regions of these cycles. In

[1]The bifurcation structure is called *period adding* when the regions associated with attracting cycles are ordered according to the Farey summation rule applied to the rotation numbers of the related cycles. That is, between the regions related to the cycles with rotation numbers $\frac{m_1}{n_1}$ and $\frac{m_2}{n_2}$ (which are Farey neighbors, i.e., $|m_1 n_2 - m_2 n_1| = 1$) there exists a region associated with the rotation number $\frac{m_1}{n_1} \oplus \frac{m_2}{n_2} = \frac{m_1+m_2}{n_1+n_2}$. Among well-known examples of a period adding structure is the Arnold tongues (see, e.g., [5]). On the other hand, the bifurcation structure is called *period incrementing* when the regions associated with attracting cycles are ordered according to the increasing by an integer k in the periods of the related attracting cycles; each two adjacent regions are either partially overlapping, that corresponds to coexistence of the related cycles, or, in a non-generic case, they are contiguous. For more detail, see [3], [1].

[7], we explain how each of these boundaries is related to a *bolder collision bifurcation*[2] (BCB for short) of the related cycle.

In the present work we consider a more general model whose dynamics are described by a 2D discontinuous piecewise linear map $F : I^2 \to I^2$, also defined by four linear contracting maps with uncoupled variables, however, their eigenvalues are real but *different*. As a result, map F can have attracting cycles with more complicated symbolic sequences, and their periodicity regions are organized in more intricate bifurcation structures. In particular, we show that in the parameter space of map F, additionally to the structures mentioned above, there are novel bifurcation structures of mixed type caused by an interplay between period incrementing and period adding structures. Moreover, we give examples of the incrementing structures having novel properties, such as overlapping of more than two periodicity regions of the same structure, or complete disconnection of the consecutive periodicity regions.

Our study belongs to the branch of the theory of nonlinear dynamical systems associated with nonsmooth discontinuous maps. Such maps quite often appear in various applied fields, when some processes, characterized by a sharp switching between the states, are modelled by piecewise smooth functions (see, e.g., [16], [4] and references therein). Among nonsmooth discontinuous maps the most studied are so-called Lorenz maps associated with Lorenz flows and defined by 1D piecewise smooth functions with one discontinuity point (see e.g., [8], [9], [11], [6], [1]). It is known that the period adding and period incrementing bifurcation structures are characteristic for the Lorenz maps. For the discontinuous maps of higher dimension much less results are obtained. See, for example, [13], [15], where bifurcation structures in 2D discontinuous maps are studied and, in particular, it is shown that period adding and period incrementing structures can also be observed in maps of this class.

The paper is organized as follows. In Sec.2 we recall the Matsuyama fashion cycle model formulated in continuous time in [12], whose discrete time analogue is considered in [7]. Then in Sec.3 we introduce a generalized fashion cycle model in discrete time, whose dynamics are defined by map F. In Sec.4 we list some properties of map F and propose an overview of the bifurcation structure of its parameter space, illustrated by 2D bifurcation diagrams and by several examples of coexisting attracting cycles together with their basins. In Sec.5 we describe period incrementing structures associated with symmetric and asymmetric cycles, noticing several distinctive properties of these structures, and in Sec.6 we explain a mechanism of creation of more complicated bifurcation structures of mixed type. We conclude in Sec.7.

2 The Matsuyama (1992) Fashion Cycle Model

What is the *fashion cycle*? In [12], it is defined as a collective process of continuous change, in which certain forms of social behavior, or "styles", enjoy temporary popularity only to be replaced by others. This pattern of change sets the fashion cycle apart from the *social custom*. And it is argued that, in order for such recurrent patterns of the fashion cycle to emerge, two fundamentally irreconcilable desires of human beings – *Conformity* (i.e., one's desire to act or look the same as others) and *Nonconformity* (one's desire to act or look different from others) – both must operate. Conformity *alone* would lead to an emergence of the social custom, or convention. Nonconformity *alone* would prevent any discernible patterns from emerging. What is necessary for an emergence of the fashion cycle is a balance between Conformity and Nonconformity.

To capture this idea and to study the social environment that leads to fashion cycles as opposed to social customs, [12] considers the society populated by two types of anonymous players, *Conformists* and *Nonconformists*, who play the following dynamic game in continuous time, $t \in [0, \infty)$.

- Each player is continuously matched with another player of either type with some probability. The relative frequency of across-type versus within-type matchings is $m > 0$ for a Conformist and $m^* > 0$ for a Nonconformist.[3]

[2] A border collision bifurcation occurs if an invariant set of a nonsmooth map collides with a border (called also a switching manifold) under variation of some parameter, that leads to a sharp change of the dynamics of the map. A switching manifold is a set which separates the regions of different definition of the map. See, e.g., [14], [4], [1].

[3] These relative frequencies of across-type versus within-type matchings for each type are in turn determined by the relative size of the two types and the relative frequency of the matching being inter-type versus intra-type.

- Each player takes one of the two actions, A and B, and the opportunity to switch actions follows as an independent, identical Poisson process, whose mean arrival rate is $\alpha > 0$.
- When matched, a Conformist gains a *higher* payoff if he sees his matched partner has the same action with his, instead of the different action. A Nonconformist, on the other hand, gains a *lower* payoff if she sees her matched partner takes the same action with her, instead of the different action.

Let $\lambda_t(\lambda_t^*) \in [0,1]$ denote the fraction of Conformists (Nonconformist) with A at time t. Then, it is more likely for a Conformist to be matched with someone with A, if $P_t \equiv (\lambda_t - 1/2) + m(\lambda_t^* - 1/2) > 0$, in which case, the fraction $1 - \lambda_t$ of the Conformists who are currently with B switch to A when the opportunity to switch actions arrives, which follows the Poisson process with the mean arrival rate $\alpha > 0$. Thus, λ_t changes as $\frac{d\lambda_t}{dt} = \alpha(1 - \lambda_t)$ if $P_t > 0$. On the other hand, it is more likely for a Nonconformist to be matched with someone with A, if $P_t^* \equiv m^*(\lambda_t - 1/2) + (\lambda_t^* - 1/2) > 0$, in which case, the fraction λ_t^* of the Nonconformists who are currently with A would switch to B, when the opportunity to switch arrives, so that λ_t^* changes as $\frac{d\lambda_t^*}{dt} = -\alpha\lambda_t^*$ if $P_t^* < 0$. Following this line of logic, the dynamics of $(\lambda_t, \lambda_t^*) \in [0,1]^2$ can be described by the following dynamical system denoted Λ:

$$\begin{aligned}
\frac{d\lambda_t}{dt} &\in \begin{cases} \{\alpha(1-\lambda_t)\} & \text{if } P_t > 0, \\ [-\alpha\lambda_t, \alpha(1-\lambda_t)] & \text{if } P_t = 0, \\ \{-\alpha\lambda_t\} & \text{if } P_t < 0, \end{cases} \quad \text{where } P_t \equiv (\lambda_t - 1/2) + m(\lambda_t^* - 1/2) \\
\frac{d\lambda_t^*}{dt} &\in \begin{cases} \{-\alpha\lambda_t^*\}, & \text{if } P_t^* > 0, \\ [-\alpha\lambda_t^*, \alpha(1-\lambda_t^*)], & \text{if } P_t^* = 0, \\ \{\alpha(1-\lambda_t^*)\}, & \text{if } P_t^* < 0, \end{cases} \quad \text{where } P_t^* = m^*(\lambda_t - 1/2) + (\lambda_t^* - 1/2)
\end{aligned} \tag{1}$$

In [12], it is shown that this dynamical system has effectively three kinds of asymptotic behaviors, depending on the two parameters, $m > 0$ and $m^* > 0$ (see Fig.1). In particular, for $m^* > m > 1$, there exists a unique limit cycle, along which Nonconformists become fashion leaders, and switch their actions periodically, while Conformists follow with delay. In fact, this limit cycle can occur through two kinds of bifurcation. First, starting from the case of $m > m^* > 1$, where $(\lambda_t, \lambda_t^*) = (1/2, 1/2)$ is the globally attracting fixed point, an increase in the share of Conformists (a decrease in the share of Nonconformists) leads to a loss of the stability of $(\lambda_t, \lambda_t^*) = (1/2, 1/2)$, which creates the limit cycle, through a mechanism similar to a Hopf bifurcation. Second, starting from the case of $m^* > 1 > m$, where $(\lambda_t, \lambda_t^*) = (1, 0)$ and $(\lambda_t, \lambda_t^*) = (0, 1)$ are two stable fixed points, whose basins of attraction are separated by $P_0 = 0$ (this case can be interpreted as the Conformists setting the social custom, and the Nonconformists revolting against it), a decrease in the share of Conformists (an increase in the share of Nonconformists) leads to a loss of the stability of both $(\lambda_t, \lambda_t^*) = (1, 0)$ and $(\lambda_t, \lambda_t^*) = (0, 1)$, which creates the limit cycle through a nonsmooth analogue of a heteroclinic bifurcation.

3 A Generalized Fashion Cycle Model in Discrete-Time

In the present paper, we reformulate the above continuous-time fashion cycle model into a discrete-time setting as follows. Matching now takes place at a regular interval, $\triangle > 0$, and from the current match and the next match, the fraction $\delta_x = 1 - e^{-\alpha_x \triangle} > 0$ of the Conformists can switch actions before the next match, and $\delta_y = 1 - e^{-\alpha_y \triangle} > 0$ of the Nonconformists can switch actions before the next match. Then, the dynamics of a discrete version of the Matsuyama fashion cycle model can be described by a family of 2D discontinuous piecewise linear (PWL for short) maps $F : I^2 \to I^2$, $I^2 = [0,1] \times [0,1]$, given by

$$x_{i+1} = \begin{cases} (1-\delta_x)x_i + \delta_x & \text{if } P^x(x_i, y_i) > 0 \\ (1-\delta_x)x_i & \text{if } P^x(x_i, y_i) < 0 \end{cases}$$

$$y_{i+1} = \begin{cases} (1-\delta_y)y_i & \text{if } P^y(x_i, y_i) > 0 \\ (1-\delta_y)y_i + \delta_y & \text{if } P^y(x_i, y_i) < 0 \end{cases}$$

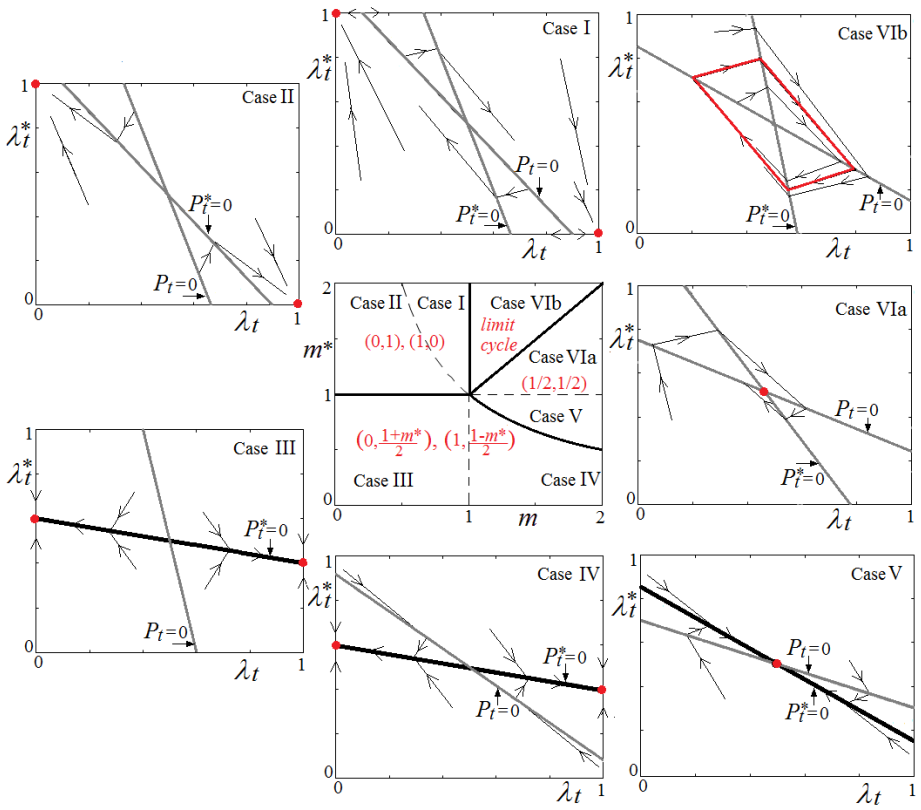

Figure 1: In the center: Partitioning of the (m, m^*)-parameter plane into the regions related to different dynamics of the continuous-time fashion cycle model Λ. Around the center: examples of the corresponding attractors of Λ.

where

$$P^x(x_i, y_i) = (x_i - 1/2) + m_x(y_i - 1/2), \quad P^y(x_i, y_i) = (y_i - 1/2) + m_y(x_i - 1/2)$$

and the parameters satisfy the following conditions:

$$\begin{array}{l} 0 < 1 - \delta_x = e^{-\alpha_x \triangle} < 1, \ 0 < 1 - \delta_y = e^{-\alpha_y \triangle} < 1 \\ m_x > 0, \ m_y > 0 \end{array} \tag{2}$$

Note that parameters $m_x > 0$, $m_y > 0$ and variables $(x_i,\, y_i) \in I^2$ correspond to parameters $m > 0$, $m^* > 0$ and variables $(\lambda_t,\, \lambda_t^*) \in I^2$, respectively, in the continuous time formulation of the model. Furthermore, this map is a generalization of the fashion cycle model in [12], which is a special case of the above, $\delta_x = \delta_y$ (or equivalently, $\alpha_x = \alpha_y$).

The discontinuity lines $P^x(x, y) = 0$ and $P^y(x, y) = 0$ divide the phase plane of map F into four regions denoted D_i, $i = \overline{1,4}$, associated with four linear maps denoted F_i :

$$\begin{array}{ll} F_1 : \begin{pmatrix} x \\ y \end{pmatrix} \mapsto \begin{pmatrix} (1-\delta_x)x \\ (1-\delta_y)y + \delta_y \end{pmatrix}, & \text{for } (x, y) \in D_1 \\ F_2 : \begin{pmatrix} x \\ y \end{pmatrix} \mapsto \begin{pmatrix} (1-\delta_x)x + \delta_x \\ (1-\delta_y)y \end{pmatrix}, & \text{for } (x, y) \in D_2 \\ F_3 : \begin{pmatrix} x \\ y \end{pmatrix} \mapsto \begin{pmatrix} (1-\delta_x)x \\ (1-\delta_y)y \end{pmatrix}, & \text{for } (x, y) \in D_3 \\ F_4 : \begin{pmatrix} x \\ y \end{pmatrix} \mapsto \begin{pmatrix} (1-\delta_x)x + \delta_x \\ (1-\delta_y)y + \delta_y \end{pmatrix}, & \text{for } (x, y) \in D_4 \end{array} \tag{3}$$

where

$$\begin{aligned} D_1 &= \{(x,y)\in I^2 : P^x(x,y)<0,\ P^y(x,y)<0\},\ D_2=\{(x,y)\in I^2 : P^x(x,y)>0,\ P^y(x,y)>0\} \\ D_3 &= \{(x,y)\in I^2 : P^x(x,y)<0,\ P^y(x,y)>0\},\ D_4=\{(x,y)\in I^2 : P^x(x,y)>0,\ P^y(x,y)<0\} \end{aligned}$$

One can immediately notice that the two variables of the map, $(x_i, y_i) \in I^2$, are connected only via the discontinuity lines $P^x(x_i, y_i) = 0$ and $P^y(x_i, y_i) = 0$.[4] Furthermore, the slopes of the linear functions defining the map, a_x, a_y, satisfy

$$0 < a_x = 1 - \delta_x < 1,\ 0 < a_y = 1 - \delta_y < 1$$

thus, map F can have neither repelling and saddle cycles, nor chaotic dynamics. Nevertheless, the bifurcation structure of the parameter space of map F, associated with its attracting cycles, is quite intricate. In [7], which considers the case of $\delta_x = \delta_y$, it is shown that the periodicity regions related to attracting cycles of different periods are organized in the period adding and period incrementing bifurcation structures; the boundaries of all the periodicity regions, corresponding to BCBs of the related cycles, are obtained in explicit form. In the present paper we show that for $\delta_x > \delta_y$, the structures mentioned above also exist, but in addition, there exists a greater variety of possible symbolic sequences, the incrementing structures have distinctive properties, moreover, we describe the novel bifurcation structures of mixed type which cannot be observed for $\delta_x = \delta_y$. The case $\delta_x < \delta_y$ is left for the future study.

4 Preliminaries

Let us rewrite the border lines $P^x(x, y) = 0$ and $P^y(x, y) = 0$ as

$$C^x:\quad y=-\frac{1}{m_x}\left(x-\frac{1}{2}\right)+\frac{1}{2},\qquad C^y:\quad y=-m_y\left(x-\frac{1}{2}\right)+\frac{1}{2} \tag{4}$$

These lines are symmetric *with respect to* (*wrt* for short) the intersection point $S = \left(\frac{1}{2}, \frac{1}{2}\right)$, and coincide if

$$C:\qquad m_y=\frac{1}{m_x} \tag{5}$$

in which case map F is defined by the functions F_1 and F_2 only. It is immediate the following

Property 1 *Map F is symmetric wrt point S and, thus, any invariant set A of map F is either symmetric wrt S or there exists one more invariant set A' which is symmetric to A wrt S.*

Let the fixed points of maps F_i, $i = \overline{1,4}$, be denoted P_i^*, so that

$$P_1^*:(x,y)=(0,1),\ P_2^*:(x,y)=(1,0),\ P_3^*:(x,y)=(0,0),\ P_4^*:(x,y)=(1,1) \tag{6}$$

Similar to the case $\delta_x = \delta_y$ described in [7], for $\delta_x > \delta_y$ map F can have *border* and *interior* cycles. Border cycles, if they exist, are located on the left and right borders of I^2 denoted I_0 and I_1, respectively. A border n-cycle, $n \geq 2$, belonging to I_0 is denoted as $\gamma_n = \{(0, y_i)\}_{i=0}^{n-1}$; Property 1 implies that such a cycle necessarily coexists with the symmetric n-cycle $\gamma'_n = \{(1, 1 - y_i)\}_{i=0}^{n-1} \in I_1$. An interior n-cycle is denoted as $\Gamma_n = \{p_i\}_{i=0}^{n-1} = \{(x_i, y_i)\}_{i=0}^{n-1}$, $n \geq 2$. From Property 1 it follows that if the n is odd there must exist also a symmetric n-cycle $\Gamma'_n = \{p'_i\}_{i=0}^{n-1} = \{(1 - x_i, 1 - y_i)\}_{i=0}^{n-1}$, while a cycle of even period may be unique if it is symmetric wrt S.

To distinguish between different interior cycles of the same period, we represent an interior cycle by a symbolic sequence $\sigma = \sigma_0\sigma_1...\sigma_{n-1}$ where $\sigma_i \in \{\mathbf{1}, \mathbf{2}, \mathbf{3}, \mathbf{4}\}$ and

$$\sigma_i=\begin{cases}\mathbf{1} & \text{if } p_i\in D_1\\ \mathbf{2} & \text{if } p_i\in D_2\\ \mathbf{3} & \text{if } p_i\in D_3\\ \mathbf{4} & \text{if } p_i\in D_4\end{cases}$$

[4] Note that map F is not defined at the discontinuity lines. In fact, such a definition does not influences the overall bifurcation structure of the parameter space which is the main subject of our study. What is really important for the bifurcation analysis are the limit values of the system function on both sides of the borders.

To simplify the notation, in some cases we will denote a cycle by its symbolic sequence. Note that from the linearity of maps F_i, $i = \overline{1,4}$, it follows that map F cannot have two different cycles with the same symbolic sequence.

Property 2 *Let $p_0 = (x_0, y_0) \in D_i$, $i = \overline{1,4}$, then the consecutive points $p_j = F_i^j(p_0) \in D_i$, $j \geq 1$, belong to the following invariant curves:*

$$\begin{array}{ll} y = (y_0 - 1)\left(\frac{x}{x_0}\right)^r + 1 & \text{if } p_0 \in D_1 \\ y = y_0\left(\frac{x-1}{x_0-1}\right)^r & \text{if } p_0 \in D_2 \\ y = y_0\left(\frac{x}{x_0}\right)^r & \text{if } p_0 \in D_3 \\ y = (y_0 - 1)\left(\frac{x-1}{x_0-1}\right)^r + 1 & \text{if } p_0 \in D_4 \end{array} \tag{7}$$

where

$$r = \log_{a_x} a_y = \frac{\ln a_y}{\ln a_x},\ 0 < r < 1 \tag{8}$$

Property 2 can be easily verified as follows. First note that the inequality $0 < r < 1$ follows from $0 < \delta_y < \delta_x < 0$, or $0 < a_x < a_y < 1$ (for $\delta_x = \delta_y$ it holds that $r = 1$, that is, the related invariant curves are straight lines). Let us take an arbitrary initial point $p_0 = (x_0, y_0) \in D_1$. To this point the linear map F_1 is applied k times, $k \geq 1$, leading to a trajectory which moves along an invariant curve of map F_1 towards its fixed point P_1^*. This trajectory either enters another region or converges to the fixed point of F_1. It obviously holds that point $(x_j, y_j) = F_1^j(x_0, y_0)$ is given by

$$\left\{ \begin{array}{l} x_j = x_0 a_x^j \\ y_j = (y_0 - 1)a_y^j + 1 \end{array} \right. \quad \text{for } 1 \leq j < k$$

Extracting power j from the first equation and substituting it to the second one, we get that $y_j = (y_0 - 1)\left(\frac{x_j}{x_0}\right)^r + 1$, where $r = \log_{a_x} a_y$, that is, the consecutive points $p_j \in D_1$ of the trajectory satisfy the equation $y = (y_0 - 1)\left(\frac{x}{x_0}\right)^r + 1$ defining the invariant curve of map F_1 passing through the point $p_0 \in D_1$. The other curves in (7) are obtained in a similar way taking into account the other linear maps F_2, F_3 and F_4.

From Property 2 it follows that the consecutive periodic points of an interior cycle Γ_n, located in a region D_i, belong to the corresponding invariant curve of map F_i, $i = \overline{1,4}$. As examples, see the 10-cycles $\mathbf{1}^5\mathbf{2}^4\mathbf{3}^1$ and $\mathbf{2}^5\mathbf{1}^4\mathbf{4}^1$, symmetric to each other, or a symmetric 14-cycle $\mathbf{1}^3\mathbf{3}^1\mathbf{1}^3\mathbf{2}^3\mathbf{4}^1\mathbf{2}^3$, which are shown in Fig.2a and Fig.2b, respectively, together with the related invariant curves of maps F_i.

As in the case $\delta_x = \delta_y$ (see [7]), for $\delta_x > \delta_y$ the (m_x, m_y)-parameter plane of map F can be subdivided into 6 regions R_i, $i = \overline{I, VI}$, depending on $m_x m_y \gtrless 1$ and $m_x \gtrless 1$, $m_y \gtrless 1$ (see the center of Fig.3): $R_I = \{m_x < 1, m_x m_y < 1\}$, $R_{II} = \{m_y > 1, m_x m_y < 1\}$, $R_{III} = \{m_x < 1, m_y < 1\}$, $R_{IV} = \{m_x > 1, m_x m_y < 1\}$, $R_V = \{m_y < 1, m_x m_y > 1\}$ and $R_{VI} = \{m_x > 1, m_y > 1\}$. To get an idea about the bifurcation structure of these regions and to compare the case $\delta_x = \delta_y$ with the case $\delta_x > \delta_y$, we show 2D bifurcation diagrams in the $(\arctan(m_x), \arctan(m_y))$-parameter plane for $\delta_x = \delta_y = 0.3$ in Fig.4a and $\delta_x = 0.5$, $\delta_y = 0.3$ in Fig.4b. In these figures, periodicity regions related to the attracting cycles of different periods are shown by different colors and some periods are indicated also by numbers. Besides the regions R_I and R_{II}, associated with the attracting fixed points, one can recognize a period adding bifurcation structure covering the whole region R_{III} and extending to region R_{IV}, as well as several period incrementing bifurcation structures in regions R_V and R_{VI}.

The dynamics associated with regions R_I, R_{II} and R_{III} (i.e., for $m_x < 1$) are relatively easy to describe:

Proposition 1 *For $(m_x, m_y) \in R_I \cup R_{II}$ and $\delta_x \geq \delta_y$, any trajectory of map F with an initial point located below or above the border line C^x converges to the fixed point P_1 or P_2, respectively.*

In fact, for the considered parameter values any trajectory with an initial point $p_0 \in D_3$ ($p_0 \in D_4$), by applying map F_3 (F_4) moves towards its fixed point $P_3^* \in D_1$ ($P_4^* \in D_2$) which is virtual for the map F because

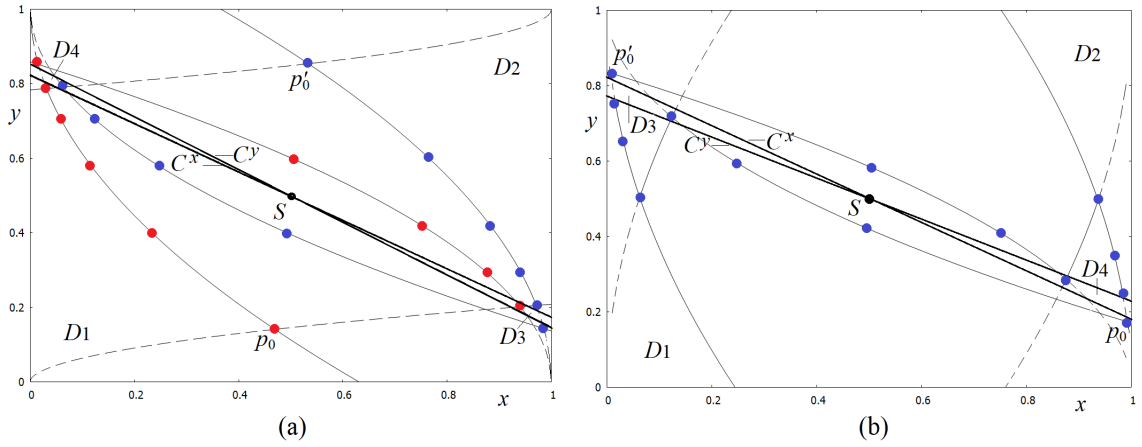

Figure 2: (a) Symmetric to each other 10-cycles $\mathbf{1}^4\mathbf{4}^1\mathbf{2}^5$ and $\mathbf{2}^4\mathbf{3}^1\mathbf{1}^5$; (b) symmetric 14-cycle $\mathbf{1}^3\mathbf{3}^1\mathbf{1}^3\mathbf{2}^3\mathbf{4}^1\mathbf{2}^3$. The related invariant curves of maps F_i, $i = \overline{1,4}$, are also shown. Here $\delta_x = 0.5$, $\delta_y = 0.3$ and (a) $(m_x, m_y) = (\tan(1), \tan(0.6)) \in R_V$; (b) $(m_x, m_y) = (\tan(1), \tan(0.5)) \in R_{IV}$.

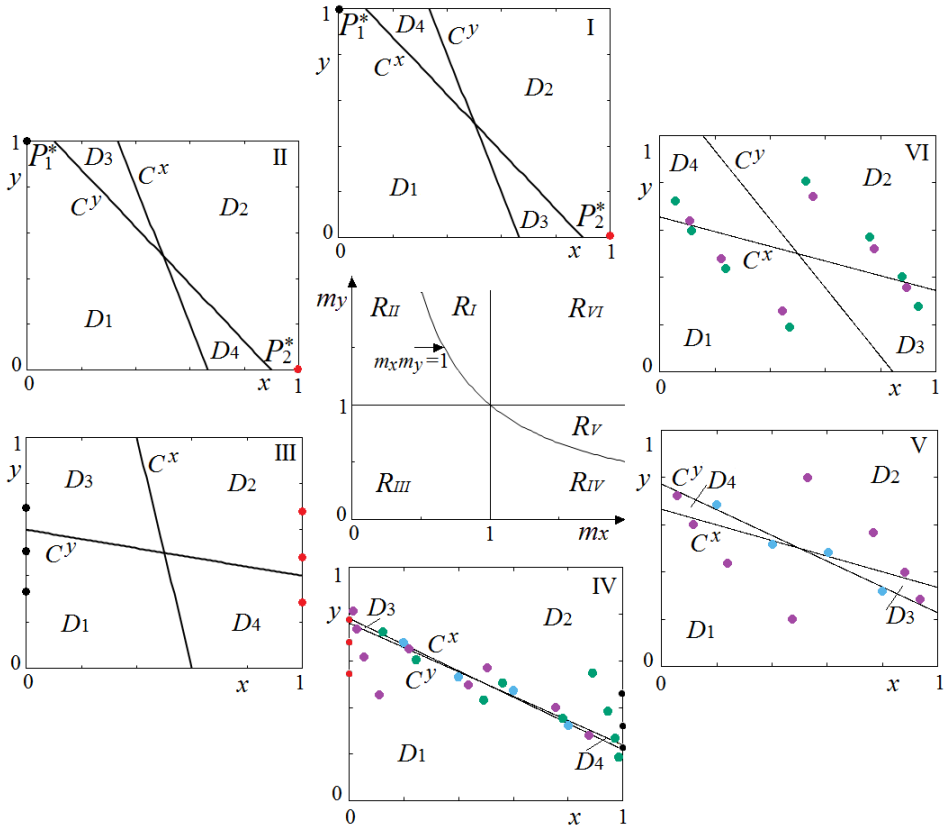

Figure 3: In the center: Partitioning of the (m_x, m_y)-parameter plane into the regions R_i, $i = \overline{I, VI}$. Around the center: examples of the corresponding attractors of map F.

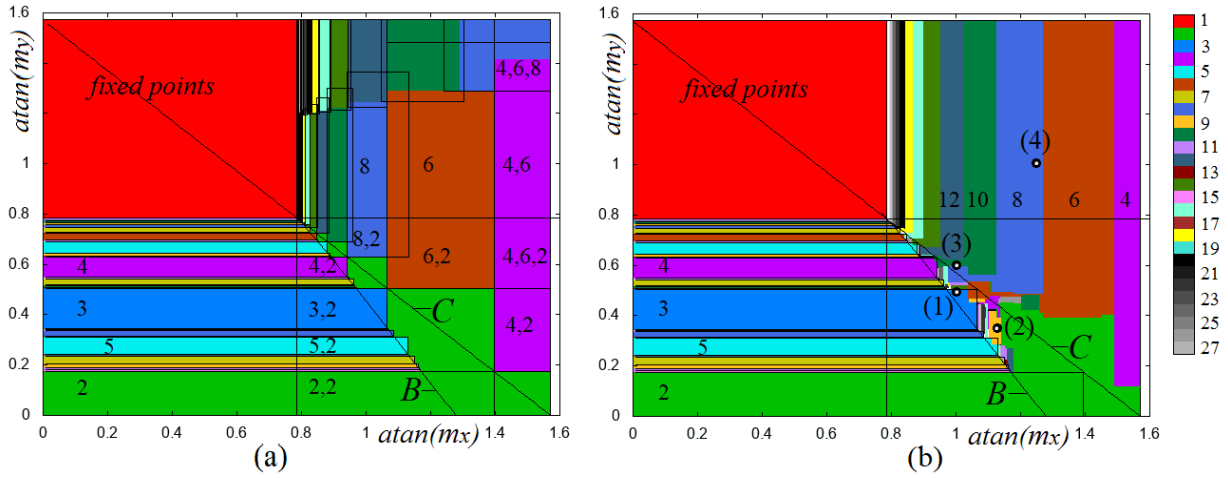

Figure 4: 2D bifurcation diagram in the $(\arctan(m_x), \arctan(m_y))$-plane of map F at (a) $\delta_x = \delta_y = 0.3$; (b) $\delta_x = 0.5$, $\delta_y = 0.3$. Attracting cycles and their basins, associated with the parameter points marked (1)-(4) in (b) are show in Fig.5a-d, respectively.

it doesn't belong to the proper definition region (see the figures marked I and II in Fig.3). Thus, the trajectory necessarily enters region D_1 (D_2). Then applying F_1 (F_2) the trajectory necessarily converges to its fixed point $P_1^* \in D_1$ ($P_2^* \in D_2$) because for $\delta_x \geq \delta_y$ (so that $r \leq 1$, see (8)) the corresponding invariant curve of map F_1 (F_2), along which the trajectory moves (see (7)), cannot intersect the discontinuity lines, that is, the trajectory cannot come back to region D_3 (D_4).

Proposition 2 *For $(m_x, m_y) \in R_{III}$ and $\delta_x \geq \delta_y$, any trajectory of map F with an initial point located below (above) the discontinuity line C^x converges either to a border n-cycle $\gamma_n \in I_0$ ($\gamma'_n \in I_1$), $n \geq 2$, or, in a non-generic case, to a Cantor set attractor $q_\rho \in I_0$ ($q'_\rho \in I_1$). The asymptotic behavior of the trajectories of map F depends on the values of the parameters δ_y and m_y only; the (δ_y, m_y)-parameter plane is organized by a period adding bifurcation structure formed by the periodicity regions related to the border cycles.*

To show that any initial point located below C^x (i.e., in the region $D_1 \cup D_3$, see the figure marked III in Fig.3) converges to border I_0, one can use, as in the previous case, the inequality $r \leq 1$ which holds for $\delta_x \geq \delta_y$. In fact, following an invariant curve of map F_1 any trajectory with an initial point $p_0 \in D_1$ necessarily enters region D_3 (note that if $r > 1$ the trajectory may enter region D_2), while any trajectory with initial point $p_0 \in D_3$ necessarily enters region D_1. Given that for these regions it holds that $x_i \to 0$ as $i \to \infty$, the trajectory $\{(x_i, y_i)\}_{i \geq 0}$ converges to border I_0 on which the dynamics are governed by a 1D discontinuous PWL map $g : I_0 \to I_0$ defined as follows:

$$g : y \to g(y) = \begin{cases} g_L(y) = (1 - \delta_y)y + \delta_y, & 0 \leq y < c \\ g_R(y) = (1 - \delta_y)y, & c < y \leq 1 \end{cases} \tag{9}$$

Here the discontinuity point $c = (m_y + 1)/2$ is associated with the intersection of the discontinuity line C^y and the border I_0, namely, $C^y \cap I_0 = (0, c)$. Similarly, any initial point located above C^x (i.e., in region $D_2 \cup D_4$) converges to border I_1 where the dynamics are defined by the map $g' : I_1 \to I_1$ having the same linear branches as map g and discontinuity point $c' = 1 - c$. The dynamics of the 1D discontinuous PWL maps such as g or g', are well studied (see, e.g., [10], [9], [2], [6]). Given that these maps do not depend on δ_x, the results obtained for $\delta_x = \delta_y$ hold also for $\delta_x > \delta_y$. For the detailed description of the related dynamics we refer to [7], while here we recall only that depending on the values of δ_y and m_y, map g (g') has either an attracting n-cycle $\gamma_n \in I_0$ ($\gamma'_n \in I_1$), $n \geq 2$, associated with a rational rotation number $\frac{m}{n}$, or, in a non-generic case, a Cantor set attractor $q_\rho \in I_0$ ($q'_\rho \in I_1$) related to an irrational rotation ρ. In the parameter space the periodicity regions associated

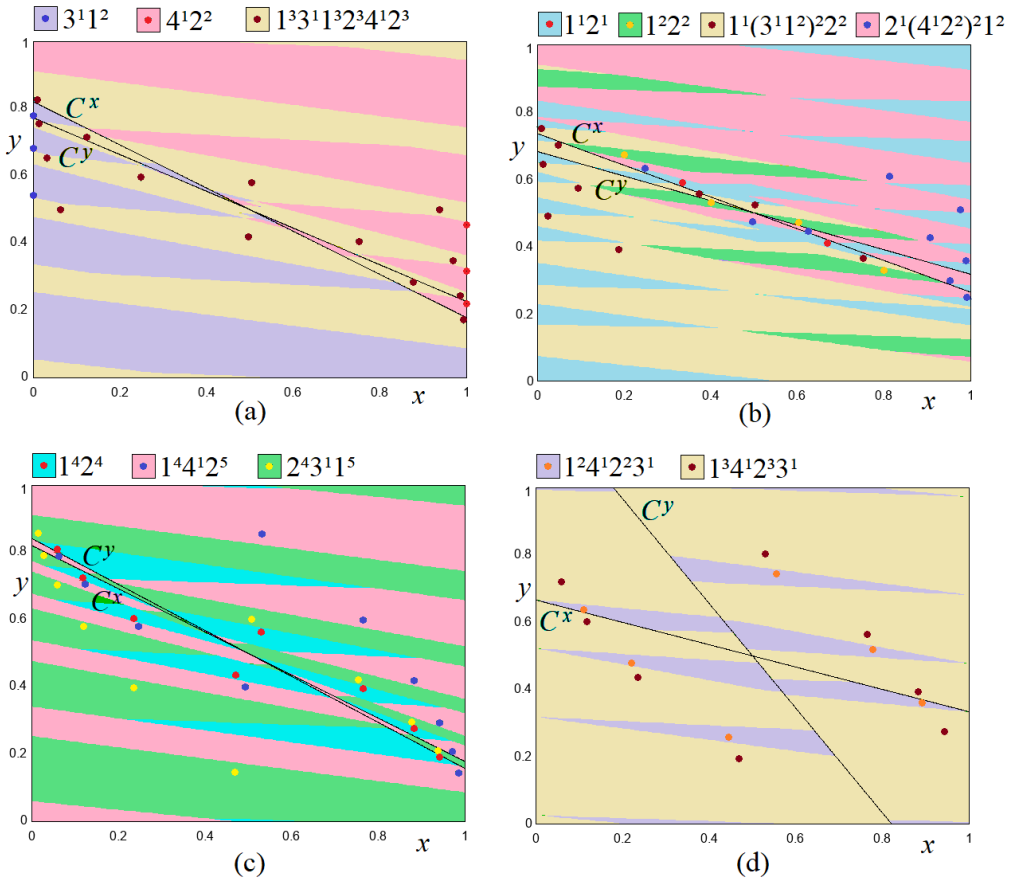

Figure 5: Cycles of map F and their basins for $\delta_x = 0.5$, $\delta_y = 0.3$ and (a) $(m_x, m_y) = (\tan(1), \tan(0.5)) \in R_{IV}$; (b) $(m_x, m_y) = (\tan(1.13), \tan(0.35)) \in R_{IV}$; (c) $(m_x, m_y) = (\tan(1), \tan(0.6)) \in R_V$; (d) $(m_x, m_y) = (\tan(1.25), \tan(1)) \in R_{VI}$. In Fig.4b corresponding parameter points are marked by (1), (2), (3) and (4), respectively.

with attracting cycles form a period adding structure; the boundaries of the periodicity regions correspond to the BCBs of the related cycles. Note that in the (m_x, m_y)-parameter plane these boundaries are horizontal lines, and in Fig.4a,b they are plotted using the related analytical expressions which can be found in [7].

The aim of the present study is to describe the dynamics of map F associated with the regions R_{IV}, R_V and R_{VI} (i.e., for $m_x > 1$). Let us first give a short description of these regions using Fig.4b as an example.

As already noticed, the period adding structure existing in region R_{III} extends to region R_{IV}. Indeed, for $(m_x, m_y) \in R_{IV}$ map F still can have border attractors which, however, can coexist with one or several interior cycles. For example, in Fig.5a two border 3-cycles coexist with one symmetric interior 14-cycle $\mathbf{1}^3\mathbf{3}^1\mathbf{1}^3\mathbf{2}^3\mathbf{4}^1\mathbf{2}^3$ (the related parameter point is marked by (1) in Fig.4b), while in Fig.5b there are only four interior cycles: 2- and 4-cycles, $\mathbf{1}^1\mathbf{2}^1$ and $\mathbf{1}^2\mathbf{2}^2$, each of which is symmetric wrt S, as well as two symmetric to each other 9-cycles, $\mathbf{1}^1(\mathbf{3}^1\mathbf{1}^2)^2\mathbf{2}^2$ and $\mathbf{2}^1(\mathbf{4}^1\mathbf{2}^2)^2\mathbf{1}^2$ (see the point marked by (2) in Fig.4b). Recall that for $\delta_x = \delta_y$ and $(m_x, m_y) \in R_{IV}$ (see Fig.4a) map F has an interior 2-cycle and cannot have other interior cycles, and this 2-cycle may coexist or not with the border attractors. In Fig.4 one can notice also that for parameter values above the curve marked B, periodicity regions forming a period adding structure become truncated by the vertical boundaries. As we have shown in [7], the curve B corresponds to a contact of the absorbing interval $[g_R(c), g_L(c)]$ of map g and one more discontinuity point $y = d$ which appears when the (m_x, m_y)-parameter point moves from region R_{III} to region R_{IV}, and the border I_0 is intersected by both the lines C^y and C^x

(see the figure marked IV in Fig.3): $C^x \cap I_0 = (0, d)$, $d = \frac{1+m_x}{2m_x}$. From $g_L(c) = d$ we get the equation of the bifurcation curve B :

$$B: \qquad m_y = \frac{1 - \delta_y m_x}{m_x(1 - \delta_y)} \tag{10}$$

The vertical boundaries of the periodicity regions mentioned above correspond to the collision of a periodic point of the related border cycle with the discontinuity point $y = d$; the analytical expressions of these boundaries can also be found in [7].

If the (m_x, m_y)-parameter point moves from region R_{IV} to region R_V crossing the curve C given in (5), the discontinuity lines C^x and C^y are merging and switching their position wrt each other (see the figure marked V in Fig.3). As a result, for $(m_x, m_y) \in R_V$ map F can no longer have border attractors but only interior cycles. See, for example, Fig.5c where two interior 10-cycles, $\mathbf{1}^4\mathbf{4}^1\mathbf{2}^5$ and $\mathbf{2}^4\mathbf{3}^1\mathbf{1}^5$, symmetric to each other, coexist with the symmetric 8-cycle $\mathbf{1}^4\mathbf{2}^4$ (the related parameter point is marked (3) in Fig.4b). Recall that for $\delta_x = \delta_y$ and $(m_x, m_y) \in R_V$ (see Fig.4a) map F has an interior 2-cycle $\mathbf{1}^1\mathbf{2}^1$ which may coexist or not with one or two interior cycles having symbolic sequences $\mathbf{1}^k\mathbf{4}^1\mathbf{2}^k\mathbf{3}^1$, $k \geq 1$, and no other interior cycles can exist.

For $(m_x, m_y) \in R_{VI}$ map F has one or several interior cycles. As an example, coexisting 6- and 8-cycles $\mathbf{1}^2\mathbf{4}^1\mathbf{2}^2\mathbf{3}^1$ and $\mathbf{1}^3\mathbf{4}^1\mathbf{2}^3\mathbf{3}^1$ are shown in Fig.5d (the related parameter point is marked (4) in Fig.4b). Similar to the case $\delta_x = \delta_y$, for $\delta_x > \delta_y$ the periodicity regions in R_{VI} are associated with cycles $\mathbf{1}^k\mathbf{4}^l\mathbf{2}^k\mathbf{3}^l$, $k \geq l$, $1 \leq l \leq \bar{l}$ where $\bar{l}$ is given in (15) (see Property 4), and these regions form $\bar{l}$ period incrementing bifurcation structures which are partially overlapping. However, differently from the standard period incrementing structure, where at most two regions are overlapping, for $\delta_x > \delta_y$ more then two regions of the same incrementing structure can overlap.

In the next sections we describe in more details the interior cycles of F and the related bifurcation structures.

5 Period incrementing structures

Let $m_x > 1$, that is, we consider the regions R_{IV}, R_V and R_{VI} (see Fig.3).

5.1 Symmetric cycles

Suppose map F has an interior *symmetric* cycle Γ_n, $n \geq 2$ (thus, since the cycle is symmetric, n is even). Let p_0 be the rightmost point of Γ_n in region D_1, then the symmetric point $p_0' \in D_2$ is also a point of this cycle. The simplest cases related to the point $p_k = F_1^k(p_0)$, $k \geq 1$, where k is the first integer such that $F_1^k(p_0) \notin D_1$, are the following:

(1) Let $p_k \in D_2$. It is possible only if $(m_x, m_y) \in R_{IV}$ or $(m_x, m_y) \in R_V$. Suppose also that $p_k = p_0'$ (as, e.g., in Fig.6a). Then the symbolic sequence of cycle Γ_n is $\mathbf{1}^k\mathbf{2}^k$, $k \geq 1$, $n = 2k$. It is easy to see that in such a case there is a uniquely defined loop formed by the invariant curve of map F_1 through p_0 and the symmetric to it invariant curve of map F_2 through p_0'. The points p_0 and p_0' are the intersection points of these two curves to which all the other points of the cycle also belong.

(2) Let $p_k \in D_4$. It is not possible if $(m_x, m_y) \in R_{IV}$, it may occur if $(m_x, m_y) \in R_V$ and necessarily occurs if $(m_x, m_y) \in R_{VI}$. Then after $l \geq 1$ iterations by F_4 we get a point $p_{k+l} = F_4^l(F_1^k(p_0)) \in D_2$. Suppose that $p_{k+l} = p_0'$ (as, e.g., in Fig.6b), then the symbolic sequence of cycle Γ_n is $\mathbf{1}^k\mathbf{4}^l\mathbf{2}^k\mathbf{3}^l$, $n = 2(k+l)$. All the points of such a cycle belong to a piecewise smooth closed curve with corner points p_0, p_k, $p_{k+l} = p_0'$, $p_{2k+l} = p_k'$, formed by the invariant curves of F_i, $i = \overline{1,4}$, through the related points. It can be shown that for $(m_x, m_y) \in R_{VI}$ the only possible symbolic sequence of a cycle of map F is $\mathbf{1}^k\mathbf{4}^l\mathbf{2}^k\mathbf{3}^l$.

It is easy to verify the following

Property 3 *The rightmost point $p_0 \in D_1$ of the cycle $\mathbf{1}^k\mathbf{4}^l\mathbf{2}^k\mathbf{3}^l$, $k \geq l$, $1 \leq l \leq \bar{l}$, where $\bar{l}$ is given in (15), has the following coordinates:*

$$p_0 = (x_0, y_0) = \left(\frac{a_x^l}{1 + a_x^{l+k}}, \frac{a_y^{l+k}}{1 + a_y^{l+k}} \right) \tag{11}$$

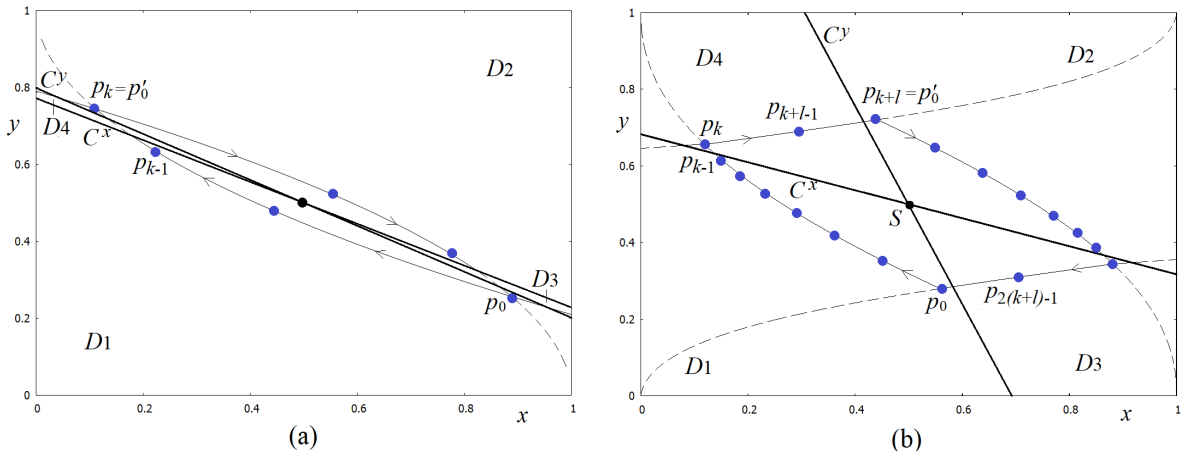

Figure 6: (a) 6-cycle $\mathbf{1}^3\mathbf{2}^3$ for $\delta_x = 0.5$, $\delta_y = 0.3$ and $(m_x, m_y) = (\tan(1.07), \tan(0.54)) \in R_V$; (b) 18-cycle $\mathbf{1}^7\mathbf{4}^2\mathbf{2}^7\mathbf{3}^2$ for $\delta_x = 0.2$, $\delta_y = 0.1$ and $(m_x, m_y) = (\tan(1.22), \tan(1.2) \in R_{VI}$. The related invariant curves of maps F_i, $i = \overline{1,4}$, are also shown.

and the rightmost point $p_0 \in D_1$ of the cycle $\mathbf{1}^k\mathbf{2}^k$, $k \geq 1$, is given by

$$p_0 = (x_0, y_0) = \left(\frac{1}{1+a_x^k}, \frac{a_y^k}{1+a_y^k} \right) \tag{12}$$

Let the periodicity region in the (m_x, m_y)-parameter plane, related to the cycle $\mathbf{1}^k\mathbf{2}^k$, be denoted as $P_{0,k}$, and to the cycle $\mathbf{1}^k\mathbf{4}^l\mathbf{2}^k\mathbf{3}^l$ as $P_{l,k}$.

Proposition 3 *For $0 < \delta_y < \delta_x < 1$, in the (m_x, m_y)-parameter plane of map F given in (3) the periodicity region $P_{0,k}$ of the cycle $\Gamma_{2k} = \{p_i\}_{i=0}^{2k-1}$ with symbolic sequence $\mathbf{1}^k\mathbf{2}^k$, $k \geq 2$, is a polygon confined by the following boundaries associated with the BCBs of Γ_{2k}:*

$$\begin{array}{lll} B^1_{0,k}: & m_y = \frac{(1-a_y^k)(1+a_x^k)}{(1-a_x^k)(1+a_y^k)} \equiv m^1_{y(0,k)} & (p_0 \in C^y) \\ B^2_{0,k}: & m_y = \frac{(a_y^{k-1}(2-a_y)-1)(1+a_x^k)}{(a_x^{k-1}(2-a_x)-1)(1+a_y^k)} \equiv m^2_{y(0,k)} & (p_{k-1} \in C^y) \\ B^3_{0,k}: & m_x = \frac{1}{m^1_{y(0,k)}} \equiv m^3_{x(0,k)} & (p_0 \in C^x) \\ B^4_{0,k}: & m_x = \frac{1}{m^2_{y(0,k)}} \equiv m^4_{x(0,k)} & (p_{k-1} \in C^x) \end{array} \tag{13}$$

where $B^1_{0,k}$, $B^2_{0,k}$, $B^3_{0,k}$ and $B^4_{0,k}$ are upper, lower, left and right boundaries of $P_{0,k}$; the region $P_{0,1}$ related to the 2-cycle $\mathbf{1}^1\mathbf{2}^1$ is two-side unbounded being confined by

$$\begin{array}{lll} B^1_{0,1}: & m_y = \frac{(1+a_x)(1-a_y)}{(1-a_x)(1+a_y)} \equiv m^1_{y(0,1)} & (p_0 \in C^x) \\ B^3_{0,1}: & m_x = \frac{1}{m^1_{y(0,1)}} \equiv m^3_{x(0,1)} & (p_0 \in C^y) \end{array}$$

namely,

$$P_{0,1} = \left\{ (m_x, m_y) : m_x > m^3_{x(0,1)},\ m_y < m^1_{y(0,1)} \right\}$$

The values defining the boundaries of $P_{0,k}$, $k \geq 2$, are obtained straightforwardly from the conditions listed in (13), where p_0 is given in (11) and

$$p_{k-1} = \left(\frac{a_x^{k-1}}{1+a_x^k}, \frac{1-a_y^{k-1}(1-a_y)}{1+a_y^k} \right)$$

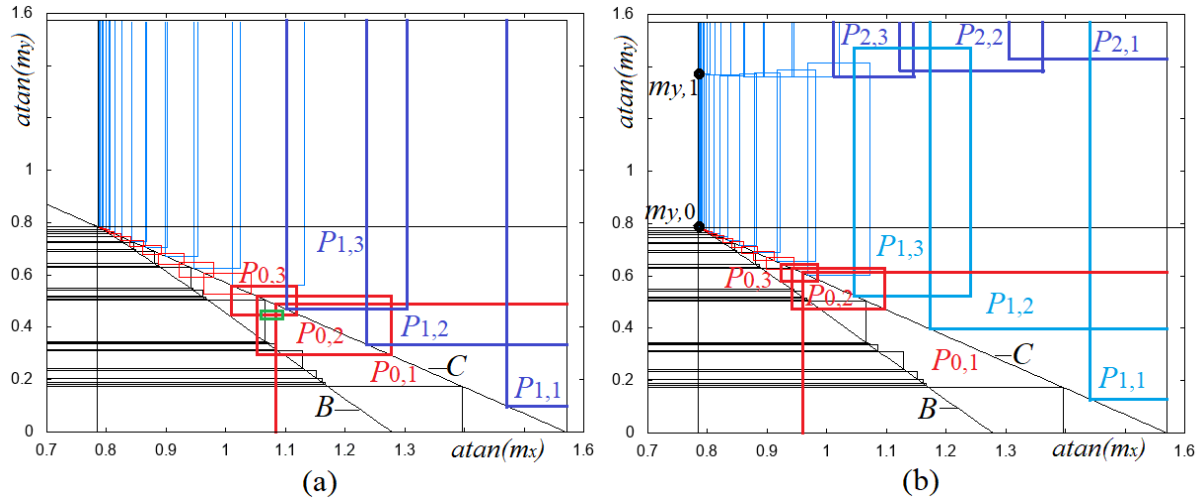

Figure 7: Boundaries of the regions $P_{l,k}$ and $P_{0,k}$ are shown in blue and red, respectively, for $\delta_y = 0.3$ and (a) $\delta_x = 0.5$, $l = \bar{l} = 1$, $k \geq 1$; (b) $\delta_x = 0.4$, $1 \leq l \leq \bar{l} = 2$, $k \geq l$. The boundaries related to the period adding structure, are shown in black. The bifurcation structure of the green rectangle in (a) is shown enlarged in Fig.10a.

The boundaries $B^1_{0,1}$ and $B^3_{0,1}$ of the region $P_{0,1}$ are obtained analogously, where p_0 is given in (12). For the considered parameter values, $m^1_{y(0,k)} > m^2_{y(0,k)}$ and $m^3_{x(0,k)} < m^4_{x(0,k)}$, $k \geq 2$, thus, in the (m_x, m_y)-parameter plane the regions $P_{0,k}$ are nonempty polygons with upper, lower, left and right boundaries $B^1_{0,k}$, $B^2_{0,k}$, $B^3_{0,k}$ and $B^4_{0,k}$, respectively:

$$P_{0,k} = \left\{(m_x, m_y) : m^3_{x(0,k)} < m_x < m^4_{x(0,k)},\ m^2_{y(0,1)} < m_y < m^1_{y(0,1)}\right\}$$

As an illustration, the boundaries of several regions $P_{0,k}$ are shown in red for $\delta_x = 0.5$, $\delta_y = 0.3$ in Fig.7a and for $\delta_x = 0.4$, $\delta_y = 0.3$ in Fig.7b. Given that $p^{1,3}_{0,k} \equiv B^1_{0,k} \cap B^3_{0,k} \in C$, $k \geq 1$, and $p^{2,4}_{0,k} \equiv B^2_{0,k} \cap B^4_{0,k} \in C$, $k \geq 2$, where the curve C is defined in (5), the boundaries $B^1_{0,k}$ and $B^4_{0,k}$ are located in region R_V, while $B^2_{0,k}$ and $B^3_{0,k}$ are in region R_{IV}.

The set $\{P_{0,k}\}_{k\geq 1}$ form a period incrementing structure with incrementing step 2, as illustrated in Fig.7, where the first three regions of this structure are emphasized. It can be shown that for fixed δ_x and δ_y, $\delta_x > \delta_y$, the regions $P_{0,k}$ shrink to the point $(m_x, m_y) = (1, 1)$ as $k \to \infty$. On the other hand, if $\delta_x - \delta_y \to 0$ (approaching the case $\delta_x = \delta_y$ described in [7]) it holds that $m^1_{y(0,1)} \to 1$ and $m^3_{x(0,1)} \to 1$, that is, the region $P_{0,1}$ tends to cover the complete region $R_{IV} \cup R_V$, while the other regions $P_{0,k}$, $k \geq 2$, move towards the point $(m_x, m_y) = (1, 1)$ shrinking in size.

The distinctive property of the period incrementing structure $\{P_{0,k}\}_{k\geq 1}$ is related to the fact that more than two periodicity regions forming this structure can be partially overlapping, as it can be seen, for example, in Fig.7 where three marked regions have a nonempty intersection. Recall that for $\delta_x = \delta_y$ the overlapping in the same incrementing structure can occur only for two adjacent regions. Differently, for $\delta_x > \delta_y$ it is possible to have coexistence also with more than two cycles whose period differs by incrementing step 2. As we discuss later, this property can be observed for other incrementing structures as well.

Proposition 4 *Let $0 < \delta_y < \delta_x < 1$. In the (m_x, m_y)-parameter plane of map F given in (3), the periodicity region $P_{l,k}$ related to the cycle $\Gamma_{2(k+l)} = \{p_i\}_{i=0}^{2(k+l)-1}$ with symbolic sequence $\mathbf{1}^k\mathbf{4}^l\mathbf{2}^k\mathbf{3}^l$, $k \geq l$, $1 \leq l \leq \bar{l}$,*

$\bar{l} = \lceil \log_{1-\delta_x} 0.5 \rceil$, *is confined by at most four boundaries associated with the BCBs of* $\Gamma_{2(k+l)}$*:*

$$\begin{array}{lll} B^1_{l,k}: & m_y = \frac{\left(1-a_y^{l+k}\right)(1+a_x^{l+k})}{(a_x^l(2-a_x^k)-1)(1+a_y^{l+k})} \equiv m^1_{y(l,k)} & (p_0 \in C^y) \\ B^2_{l,k}: & m_y = \frac{(a_y^{l+k-1}(2-a_y)-1)(1+a_x^{l+k})}{(a_x^{l-1}(a_x^{k+1}-2)+1)(1+a_y^{l+k})} \equiv m^2_{y(l,k)} & (p_{2(k+l)-1} \in C^y) \\ B^3_{l,k}: & m_x = \frac{(1-a_x^{l+k})(1+a_y^{l+k})}{(a_y^k(a_y^l-2)+1)(1+a_x^{l+k})} \equiv m^3_{x(l,k)} & (p_k \in C^x) \\ B^4_{l,k}: & m_x = \frac{(1-a_x^{l+k-1}(2-a_x))(1+a_y^{l+k})}{(1+a_y^{k-1}(a_y^{l+1}-2))(1+a_x^{l+k})} \equiv m^4_{x(l,k)} & (p_{k-1} \in C^x) \end{array} \tag{14}$$

The region $P_{l,k}$ *can be one-side unbounded (only the boundaries* $B^1_{l,k}$*,* $B^2_{l,k}$ *and* $B^3_{l,k}$*, or* $B^2_{l,k}$*,* $B^3_{l,k}$ *and* $B^4_{l,k}$*, exist) or two-side unbounded (only the boundaries* $B^2_{l,k}$ *and* $B^3_{l,k}$ *exist). Here the boundaries* $B^1_{l,k}$*,* $B^2_{l,k}$*,* $B^3_{l,k}$ *and* $B^4_{l,k}$*, if exist, are upper, lower, left and right boundaries of* $P_{l,k}$*. All the regions* $P_{l,k}$ *are located in region* $R_V \cup R_{VI}$*.*

The proof of this Proposition is similar to the one given in [7] for $\delta_x = \delta_y$. Note only that the point p_0 is defined in (11) and the other points of the cycle $\Gamma_{2(k+l)}$ which are needed to determine the BCB boundaries of $P_{l,k}$ have the following coordinates:

$$\begin{array}{ll} p_{2(k+l)-1} = & \left(\frac{a_x^{l-1}}{1+a_x^{l+k}}, \frac{a_y^{l+k-1}}{1+a_y^{l+k}} \right) \\ p_k = & \left(\frac{a_x^{l+k}}{1+a_x^{l+k}}, \frac{1+a_y^k(a_y^l-1)}{1+a_y^{l+k}} \right) \\ p_{k-1} = & \left(\frac{a_x^{l+k-1}}{1+a_x^{l+k}}, \frac{1+a_y^{k-1}(a_y^{l+1}-1)}{1+a_y^{l+k}} \right) \end{array}$$

As an example, see Fig.6b where these points are indicated using the 18-cycle $\mathbf{1}^7\mathbf{4}^2\mathbf{2}^7\mathbf{3}^2$. Similar to the regions $P_{0,k}$, if the region $P_{l,k}$ is bounded, it is a polygon where $B^1_{l,k}$, $B^2_{l,k}$, $B^3_{l,k}$ and $B^4_{l,k}$ are its upper, lower, left and right boundaries, respectively.

In Fig.7 one can see two examples of the period incrementing bifurcation structures formed by the periodicity regions whose boundaries are shown in blue: in Fig.7a, where $\delta_x = 0.5$, $\delta_y = 0.3$, there is just one period incrementing structure, $\{P_{1,k}\}_{k\geq 1}$, and in Fig.7b, where $\delta_x = 0.4$, $\delta_y = 0.3$, two period incrementing structures can be recognized, $\{P_{1,k}\}_{k\geq 1}$ and $\{P_{2,k}\}_{k\geq 2}$ (the first three regions of each structure are emphasized).

Consider an incrementing structure $\{P_{l,k}\}_{k\geq l}$ for some fixed $l \geq 1$. It can be shown that for fixed δ_x and δ_y, $\delta_x > \delta_y$, it holds that $m^3_{x(l,k)} \to 1$, $m^4_{x(l,k)} \to 1$ as $k \to \infty$, that is, both vertical boundaries, $B^3_{l,k}$ and $B^4_{l,k}$, of the related periodicity regions tend to the border $\{m_x = 1\}$ of region R_{VI}, so that these regions shrink in size in the horizontal direction. In the meantime, $m^1_{y(l,k)} \to 1/(2a_x^l - 1) \equiv m_{y,l}$ and $m^2_{y(l,k)} \to 1/(2a_x^{l-1} - 1) = m_{y,l-1}$, that is, the lower boundaries $B^2_{l,k}$ of the periodicity regions of the incrementing structure $\{P_{l,k}\}_{k\geq l}$ converge to the same value as the upper boundaries $B^1_{l-1,k}$ of the incrementing structure $\{P_{l-1,k}\}_{k\geq l-1}$ (see, e.g. Fig.7b where the points $m_{y,0}$ and $m_{y,1}$ are indicated). Note that the inequality $m_{y,l-1} > 0$ is sufficient to state that some regions $\{P_{l,k}\}_{k\geq l}$ exist in the positive quadrant of the (m_x, m_y)-parameter plane. In particular, as $k \to \infty$ and $l = 1$ it holds that $m^2_{y(1,k)} \to m_{y,0} = 1 > 0$, that is, the full set $\{P_{1,k}\}_{k\geq 1}$ always exists, while the incrementing structures with $l \geq 2$ exist depending on the value of δ_x. Indeed, from $m_{y,l-1} > 0$ we get the inequality $l < \log_{a_x} 0.5 + 1$. So, the following property holds:

Property 4 *For fixed* δ_x *and* δ_y*,* $\delta_x > \delta_y$*, in the* (m_x, m_y)*-parameter plane of map* F *the number of the period incrementing structures* $\{P_{l,k}\}_{k\geq l}$ *is given by*

$$\bar{l} = \lceil \log_{1-\delta_x} 0.5 \rceil \tag{15}$$

that is, map F *can have cycles* $\mathbf{1}^k\mathbf{4}^l\mathbf{2}^k\mathbf{3}^l$ *where* $k \geq l$*,* $1 \leq l \leq \bar{l}$*. Here* $\lceil \cdot \rceil$ *denotes the ceiling function (that is,* $\bar{l} = \log_{1-\delta_x} 0.5$ *if this value is integer, and* $\bar{l} = \lfloor \log_{1-\delta_x} 0.5 \rfloor + 1$ *otherwise, where* $\lfloor \cdot \rfloor$ *denotes the integer part of the number).*

In particular, for $0.5 \leq \delta_x < 1$ it holds that $\bar{l} = 1$, that is, there is only one period incrementing structure $\{P_{1,k}\}_{k\geq 1}$; all the regions of this structure are unbounded from above and $P_{1,1}$ is unbounded from the right side

as well (see Fig.7a). For $\delta_x = 0.4$ there are $\bar{l} = 2$ incrementing structures, as shown in Fig.7b. The following property obviously holds:

Property 5 *As $\delta_x \to 0$ the number $\bar{l}$ of incrementing structures $\{P_{l,k}\}_{k\geq l}$ tends to infinity.*

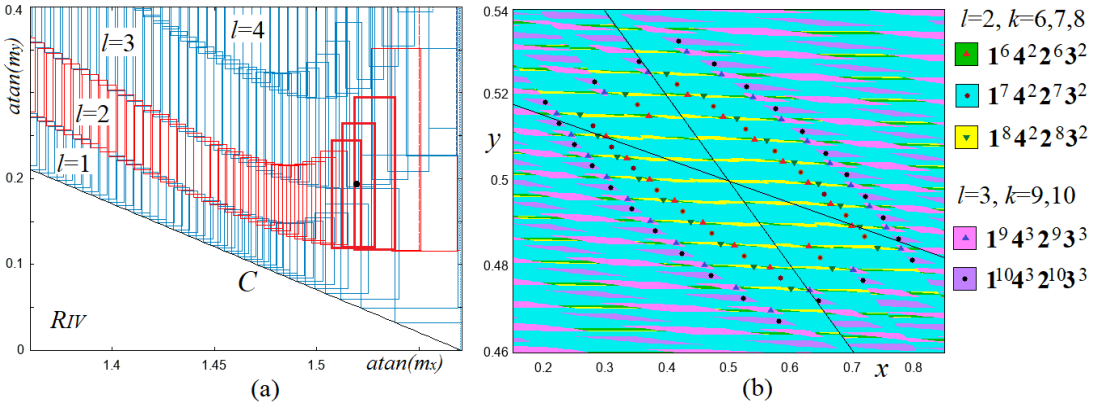

Figure 8: (a) Boundaries of the periodicity regions $\{P_{l,k}\}_{k\geq l}$ in the scaled (m_x, m_y)-parameter plane for $\delta_x = 0.1$, $\delta_y = 0.01$; (b) coexisting cycles and their basins for $(m_x, m_y) = (\tan(1.51982), \tan(0.194263)) \in R_V$ (the related parameter point is marked by black circle in (a)).

As we already mentioned, more than two periodicity regions belonging to the same incrementing structure can overlap. As an example, in Fig.8a we show an enlarged part of the scaled (m_x, m_y)-parameter plane for $\delta_x = 0.1$ (so that $\bar{l} = 7$) and $\delta_y = 0.01$, where the period incrementing structure $\{P_{2,k}\}_{k\geq 2}$ is shown in red and the three regions, $P_{2,6}$, $P_{2,7}$ and $P_{2,8}$, having an overlapping part, are emphasized. In Fig.8b coexisting cycles are shown together with their basins (the related parameter point is indicated in Fig.8a by a black circle). As one can see, there are three coexisting cycles of the same incrementing structure, namely, the cycles $\mathbf{1}^k\mathbf{4}^2\mathbf{2}^k\mathbf{3}^2$ with $k = 6, 7, 8$. Moreover, given that the incrementing structure $\{P_{2,k}\}_{k\geq 2}$ is partially overlapping with $\{P_{3,k}\}_{k\geq 3}$, in Fig.8b we see two more coexisting cycles related to this structure, namely, the cycles $\mathbf{1}^k\mathbf{4}^3\mathbf{2}^k\mathbf{3}^3$ with $k = 9, 10$. Recall that originally the period incrementing structure was described for 1D maps with one discontinuity point, and in this structure at most two periodicity regions can be overlapping, so that at most two attracting cycles can coexist (see, e.g. [6] and references therein). Since F is a map with a higher dimension and with a higher number of discontinuities, it is not surprising that more intricate bifurcation structures are observed in its parameter space, and more attractors can coexist.

To summarize, in region R_{VI} only the period incrementing structures $\{P_{l,k}\}_{k\geq l}$ are observed. The structure $\{P_{1,k}\}_{k\geq 1}$ extends also to region R_V for any $0 < \delta_y < \delta_x < 1$, given that $p^{2,3}_{1,k} \equiv B^2_{1,k} \cap B^3_{1,k} \in C$. Other incrementing structures may also extend to R_V (as e.g., in Fig.8a) depending on the values of δ_x and δ_y. As for the regions R_{IV} and R_V, it is not an easy task to describe all the possible bifurcation structures which can exist in these regions. Below we give several examples of such structures.

5.2 Asymmetric cycles

As already mentioned, map F for $\delta_x > \delta_y$, differently from the case $\delta_x = \delta_y$, can have an asymmetric interior cycle Γ_n necessarily coexisting with cycle Γ'_n which is symmetric to Γ_n wrt point S (see, e.g., Fig.2a). Let us describe the simplest bifurcation structure associated with such cycles.

Let $(m_x, m_y) \in R_V$. Suppose map F has an asymmetric interior cycle Γ_n, $n \geq 3$, and, let, as before, p_0 be the rightmost point of Γ_n in region D_1. Then the symmetric point $p'_0 \in D_2$ is a point of the cycle Γ'_n. After $k1 \geq 1$ iterations by F_1 we get a point $p_{k1} = F_1^{k1}(p_0)$, which for the considered parameter range belongs either to region D_4 or to region D_2. Let $p_{k1} \in D_4$ (then $p'_{k1} \in D_3$). There exists $l \geq 1$ such that $p_{k1+l} = F_4^l(p_{k1}) \in D_2$, and there exists also $k2 \geq 1$ such that the point $p_{k1+l+k2} = F_2^{k2}(p_{k1+l})$ belongs either to region D_1 or to region

D_3. Consider the simplest case when $l = 1$ and $p_{k1+1+k2} = p_0$. Then the symbolic sequence of the corresponding cycle Γ_n is $\mathbf{1}^{k1}\mathbf{4}^1\mathbf{2}^{k2}$, $n = k1 + k2 + 1$, and the symbolic sequence of Γ'_n is $\mathbf{2}^{k1}\mathbf{3}^1\mathbf{1}^{k2}$. It is easy to verify the following

Property 6 *The rightmost point $p_0 \in D_1$ of the cycle $\mathbf{1}^{k1}\mathbf{4}^1\mathbf{2}^{k2}$, $k1 \geq 1$, $k2 \geq 1$, has the following coordinates:*

$$p_0 = (x_0, y_0) = \left(\frac{1 - a_x^{1+k2}}{1 - a_x^{k1+1+k2}}, \frac{a_y^{k2}(1 - a_y^{k1+1})}{1 - a_y^{k1+1+k2}} \right) \tag{16}$$

and, respectively, the leftmost point $p'_0 \in D_2$ of the cycle $\mathbf{2}^{k1}\mathbf{3}^1\mathbf{1}^{k2}$ is $p'_0 = (1 - x_0, 1 - y_0)$.

Proposition 5 *Let $0 < \delta_y < \delta_x < 1$. In the (m_x, m_y)-parameter plane of map F given in (3), the periodicity region $P_{k1,k2,1}$, $k1 \geq 1$, $k2 \geq 1$, related to the coexisting cycles $\Gamma_{k1+k2+1} = \{p_i\}_{i=0}^{k1+k2}$ and $\Gamma'_{k1+k2+1} = \{p'_i\}_{i=0}^{k1+k2}$ with symbolic sequences $\mathbf{1}^{k1}\mathbf{4}^1\mathbf{2}^{k2}$ and $\mathbf{2}^{k1}\mathbf{3}^1\mathbf{1}^{k2}$, respectively, is confined by four boundaries associated with the BCBs of $\Gamma_{k1+k2+1}$:*

$$\begin{aligned}
B^1_{k1,k2,1}: \quad & m_y = \frac{\left(a_y^{k2}(2-a_y^{k1+1})-1\right)(1-a_x^{k1+1+k2})}{\left(a_x^{k2+1}(2-a_x^{k1})-1\right)(1-a_y^{k1+1+k2})} \equiv m^1_{y(k1,k2,1)} && (p_0 \in C^y) \\
B^2_{k1,k2,1}: \quad & m_y = \frac{(a_y^{k1}(2-a_y^{k2}(2-a_y))-1)(1-a_x^{k1+1+k2})}{\left(a_x^{k1}(2-a_x^{k2+1})-1\right)(1-a_y^{k1+1+k2})} \equiv m^2_{y(k1,k2,1)} && (p_{k1} \in C^y) \\
B^3_{k1,k2,1}: \quad & m_x = \frac{\left(a_x^{k1}(2-a_x^{1+k2})-1\right)(1-a_y^{k1+1+k2})}{(a_y^{k1}(2-a_y^{k2}(2-a_y))-1)(1-a_x^{k1+1+k2})} = \frac{1}{m^2_{y(k1,k2,1)}} \equiv m^3_{x(k1,k2,1)} && (p_{k1} \in C^x) \\
B^4_{k1,k2,1}: \quad & m_x = \frac{\left(a_x^{k2}(2-a_x^{k1}(2-a_x))-1\right)(1-a_y^{k1+1+k2})}{(a_y^{k2-1}(2(1-a_y^{k1+1})+a_y^{k1+2})-1)(1-a_x^{k1+1+k2})} \equiv m^4_{x(k1,k2,1)} && (p_{k1+k2} \in C^x)
\end{aligned} \tag{17}$$

The boundaries of $P_{k1,k2,1}$ are defined straightforwardly from the conditions listed in (17), where p_0 is given in (16) and

$$p_{k1} = \left(\frac{a_x^{k1}(1-a_x^{1+k2})}{1-a_x^{k1+1+k2}}, 1 - \frac{a_y^{k1}(1-a_y^{k2})}{1-a_y^{k1+1+k2}} \right)$$
$$p_{k1+k2} = \left(1 - \frac{a_x^{k2}(1-a_x^{k1})}{1-a_x^{k1+1+k2}}, \frac{a_y^{k2-1}(1-a_y^{k1+1})}{1-a_y^{k1+1+k2}} \right)$$

To state the existence of region $P_{k1,k2,1}$ for some fixed $k1 \geq 1$, $k2 \geq 1$, the conditions $0 < m^2_{y(k1,k2,1)} < m^1_{y(k1,k2,1)}$ and $0 < m^3_{x(k1,k2,1)} < m^4_{x(k1,k2,1)}$ have to be verified.

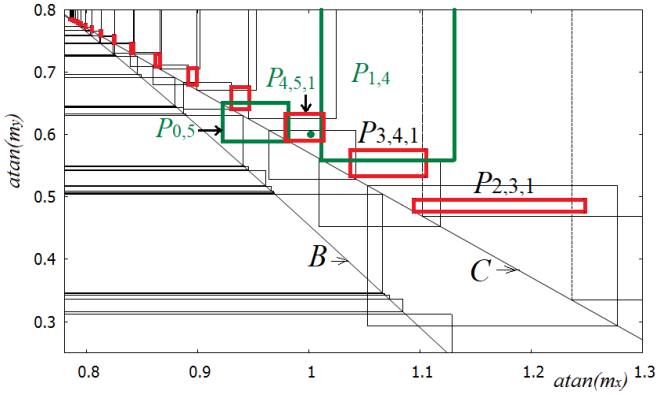

Figure 9: Period incrementing structure $\{P_{k,k+1,1}\}_{k\geq 2}$ is shown in red in the scaled (m_x, m_y)-parameter plane of map F at $\delta_x = 0.5$, $\delta_y = 0.3$. In green the 10-periodicity regions $P_{0,5}$ and $P_{1,4}$ are emphasized, belonging to the incrementing structures $\{P_{0,k}\}_{k\geq 1}$ and $\{P_{1,k}\}_{k\geq 1}$, respectively.

In Fig.9 an example of the period incrementing structure is shown in red, which is formed by the regions $P_{k1,k2,1}$ for $k1 \geq 2$ and $k2 = k1 + 1$ (one can check that $m^2_{y(1,2,1)} > m^1_{y(1,2,1)}$, while $m^2_{y(2,3,1)} < m^1_{y(2,3,1)}$,

that is, this incrementing structure starts from the region $P_{2,3,1}$). In this figure the parameter point related to the 10-cycles $\mathbf{1}^4\mathbf{4}^1\mathbf{2}^5$ and $\mathbf{2}^4\mathbf{3}^1\mathbf{1}^5$ (coexisting with the cycle $\mathbf{1}^4\mathbf{2}^4$), shown in Fig.5c, is marked by the green circle. One can notice a distinctive property of this structure: the neighbor regions are neither overlapping, nor contiguous. Each region $P_{k1,k2,1}$ is a polygon with the left lower corner belonging to the curve C, where $B^1_{k1,k2,1}$, $B^2_{k1,k2,1}$, $B^3_{k1,k2,1}$ and $B^4_{k1,k2,1}$ are its upper, lower, left and right boundaries, respectively. In Fig.9 the 10-periodicity regions $P_{0,5}$ and $P_{1,4}$, belonging to the incrementing structures described in the previous section, are shown in green, and it can be seen that the region $P_{4,5,1}$ connects these regions.

6 Mixed structures

Consider now the region R_{IV}. Recall that in this region there is a period adding structure, extending from region R_{III}, associated with the border attractors, as well as the period incrementing structure $\{P_{0,k}\}_{k\geq 1}$, extending to region R_V (see Fig.7). An interplay between these structures results in infinitely many other more complicated structures. Below we consider those which accumulate to the vertical boundaries of the periodicity regions involved in the period adding structure.

Suppose, as before, that map F has an interior cycle Γ_n, $n \geq 2$, and let p_0 be the rightmost point of Γ_n in region D_1. After $k \geq 1$ iterations by F_1 we get a point $p_k = F_1^k(p_0)$, and for $(m_x, m_y) \in R_{IV}$ it is possible that $p_k \in D_3$. Application of map F_3 necessary makes the trajectory to come back to region D_1 where map F_1 is applied again. Such alternating applications of maps F_1 and F_3 can be repeated several times, leading to the points approaching the border I_0, until the trajectory necessarily enters region D_2. If the (m_x, m_y)-parameter point is taken close enough to the vertical boundary of the periodicity region related to a border cycle, then the repeated blocks in the symbolic sequence of the corresponding interior cycle depend on the symbolic sequence of this border cycle. The closer the parameter point to the vertical border, the larger the multiplicity of the mentioned blocks, that creates a mechanism of incrementing of the period of the corresponding cycles. In such a way one can observe a mixture of the period adding and period incrementing structures.

To give an example, let us consider a neighborhood of the vertical boundary, denoted B_3, of the region involved in the period adding structure and associated with the 3-cycle $\gamma_3 \in I_0$ with symbolic sequence $\mathbf{3}^1\mathbf{1}^2$, and the 3-cycle $\gamma_3' \in I_1$ with symbolic sequence $\mathbf{4}^1\mathbf{2}^2$, symmetric to γ_3. Fig.10a presents an enlarged part of the 2D bifurcation diagram in the scaled (m_x, m_y)-parameter plane (the related window is indicated in Fig.7a by the green rectangle). From (13) it follows that in this complete window the 4-cycle $\mathbf{1}^2\mathbf{2}^2$ exists, moreover, above the boundary $B^2_{0,3}$ the 6-cycle $\mathbf{1}^3\mathbf{2}^3$ exists and to the right of the boundary $B^3_{0,1}$ the 2-cycle $\mathbf{1}^1\mathbf{2}^1$ exists. All these cycles are associated with the incrementing structure $\{P_{0,k}\}_{k\geq 1}$. Besides these regions one can recognize several period incrementing structures with incrementing steps 6 and 3, accumulating to the boundary B_3. The incrementing structures with step 3 accumulate also to the horizontal boundary of the 9-periodicity region. This region is associated with symmetric to each other 9-cycles with symbolic sequences $(\mathbf{1}^2\mathbf{3}^1)\mathbf{1}^3\mathbf{2}^3$ and $(\mathbf{2}^2\mathbf{4}^1)\mathbf{2}^3\mathbf{1}^3$, obtained by the concatenation of the symbolic sequences of the border 3-cycles with the symbolic sequence of the interior 6-cycle $\mathbf{1}^3\mathbf{2}^3$ (see Fig.10b, where these 9-cycles coexist with the 4- and 6-cycles, $\mathbf{1}^2\mathbf{2}^2$ and $\mathbf{1}^3\mathbf{2}^3$; the corresponding parameter point is indicated by the red circle in Fig.10a).

The lowest incrementing structure in Fig.10a is formed by the regions related to the cycles $\mathbf{1}^2(\mathbf{3}^1\mathbf{1}^2)^m\mathbf{2}^2(\mathbf{4}^1\mathbf{2}^2)^m$ with $m = 2, 3, ...$, accumulating to the boundary B_3. An example of coexisting 4- and 22-cycles, $\mathbf{1}^2\mathbf{2}^2$ and $\mathbf{1}^2(\mathbf{3}^1\mathbf{1}^2)^3\mathbf{2}^2(\mathbf{4}^1\mathbf{2}^2)^3$, is shown in Fig.11a (the related parameter point is indicated in Fig.10a by the gray circle). In this example the 22-cycle is symmetric, and in its symbolic sequence the blocks $\mathbf{1}^2$ and $\mathbf{2}^2$, associated with the 4-cycle $\mathbf{1}^2\mathbf{2}^2$, are followed, respectively, by the blocks $\mathbf{3}^1\mathbf{1}^2$ and $\mathbf{4}^1\mathbf{2}^2$ of multiplicity $m = 3$. In such a way the elements of incrementing and adding structures become mixed. Decreasing m_x the discontinuity line C^x becomes steeper leading to increasing multiplicity of the blocks $\mathbf{3}^1\mathbf{1}^2$ and $\mathbf{4}^1\mathbf{2}^2$.

In Fig.10a between the 22- and 9-periodicity regions (recall that the 9-periodicity region is related to two 9-cycles, of total period 18) there is a 40-periodicity region, that is, in this case the period adding rule is applied. An example of the 40-cycle is show in Fig.11b (see the green circle in Fig.10a), and its symbolic sequence $\underline{(\mathbf{1}^2\mathbf{3}^1)\mathbf{1}^3\mathbf{2}^3}\mathbf{1}^2(\mathbf{3}^1\mathbf{1}^2)^3\underline{(\mathbf{2}^2\mathbf{4}^1)\mathbf{2}^3\mathbf{1}^3}\mathbf{2}^2(\mathbf{4}^1\mathbf{2}^2)^3$ consists of the symbolic sequences of two 9-cycles (see the emphasized blocks) incorporated into the symbolic sequence of the 22-cycle. The 40-periodicity region belongs to one more incrementing structure with step 6, accumulating to the boundary B_3. This structure is associated with symbolic sequences $\underline{(\mathbf{1}^2\mathbf{3}^1)\mathbf{1}^3\mathbf{2}^3}\mathbf{1}^2(\mathbf{3}^1\mathbf{1}^2)^m\underline{(\mathbf{2}^2\mathbf{4}^1)\mathbf{2}^3\mathbf{1}^3}\mathbf{2}^2(\mathbf{4}^1\mathbf{2}^2)^m$, where $m = 2, 3, ...$.

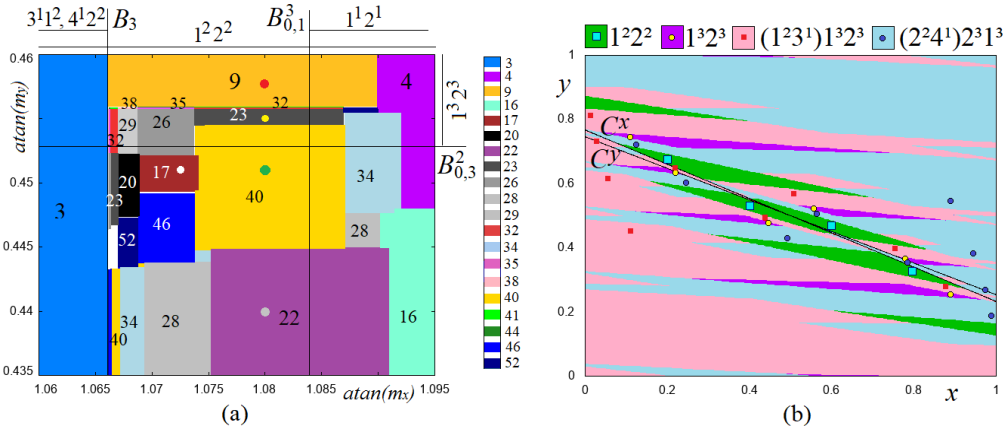

Figure 10: (a) An enlarged part of the 2D bifurcation diagram in the scaled (m_x, m_y)-parameter plane of map F at $\delta_x = 0.5$, $\delta_y = 0.3$ (see the green rectangle in Fig.7a). The numbers indicate the periods of the related cycles; (b) basins of 4- and 6-cycles, $\mathbf{1^2 2^2}$ and $\mathbf{1^3 2^3}$, coexisting with two symmetric to each other 9-cycles $(\mathbf{1^2 3^1})\mathbf{1^3 2^3}$ and $(\mathbf{2^2 4^1})\mathbf{2^3 1^3}$ for $(m_x, m_y) = (\tan(1.08), \tan(0.44))$ (the corresponding parameter point is marked by red circle in (a)).

In Fig.10a one can also recognize several incrementing structures with step 3. The structure which starts with the 17-periodicity region and accumulates to the boundary B_3, is formed by the regions of coexisting symmetric to each other cycles $\mathbf{1^2}(\mathbf{3^1 1^2})^m \mathbf{2^3}$ and $\mathbf{2^2}(\mathbf{4^1 2^2})^m \mathbf{1^3}$ with $m = 4, 5, \ldots$. Fig.12a shows these cycles in case $m = 4$ (the related parameter point is marked by the white circle in Fig.10a). One more period incrementing structure with incrementing step 3, which is close to the horizontal boundary of the 9-periodicity region and starts with the 23-periodicity region, is formed by the regions of symmetric to each other cycles $\mathbf{1^2}(\mathbf{3^1 1^2})^m \mathbf{2^3}\underline{(\mathbf{1^2 3^1})\mathbf{1^3 2^3}}$ and $\mathbf{2^2}(\mathbf{4^1 2^2})^m \mathbf{1^3}\underline{(\mathbf{2^2 4^1})\mathbf{2^3 1^3}}$, where $m = 3, 4, \ldots$ (here the emphasized blocks, as before, are symbolic sequences of the 9-cycles). Fig.12b shows these cycles in the case $m = 3$, coexisting with the cycles $\mathbf{1^2 2^2}$ and $\mathbf{1^3 2^3}$ (the related parameter point is marked by yellow circle in Fig.10a).

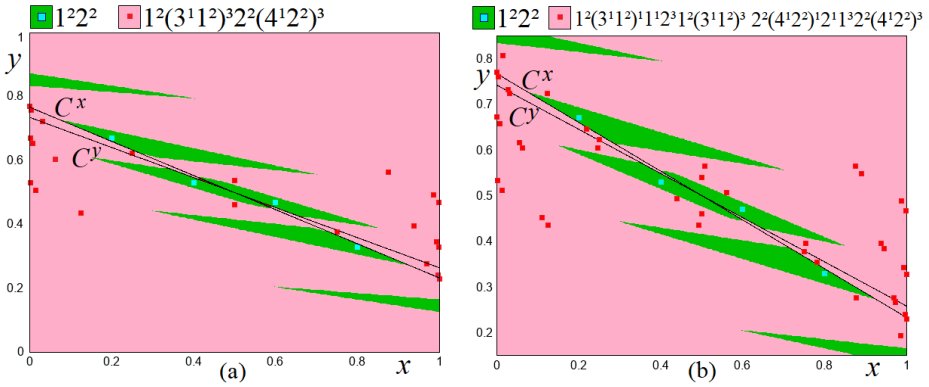

Figure 11: The basins of the 4-cycle $\mathbf{1^2 2^2}$ coexisting with (a) 22-cycle $\mathbf{1^2}(\mathbf{3^1 1^2})^3 \mathbf{2^2}(\mathbf{4^1 2^2})^3$ and (b) 40-cycle $\mathbf{1^2}(\mathbf{3^1 1^2})^1 \mathbf{1^1 2^3}$ $\mathbf{1^2}(\mathbf{3^1 1^2})^3$ $\mathbf{2^2}(\mathbf{4^1 2^2})^1 \mathbf{2^1 1^3 2^2}(\mathbf{4^1 2^2})^3$. Here (a) $(m_x, m_y) = (\tan(1.08), \tan(0.44))$; (b) $(m_x, m_y) = (\tan(1.08), \tan(0.451))$; see the gray and green circles, respectively, in Fig.10a.

Clearly, bifurcation structures similar to those described above, can exist in a neighborhood of the vertical boundary of any periodicity region involved in the period adding structure. The examples here presented

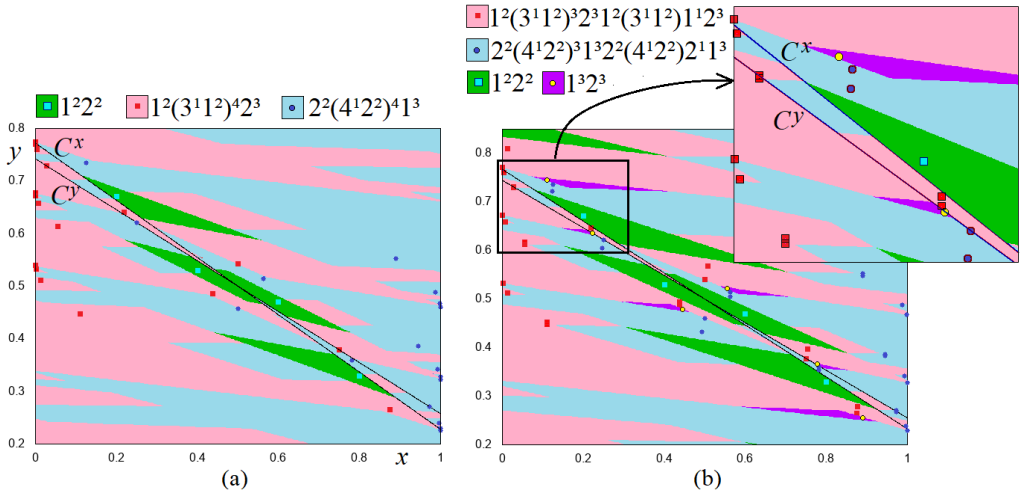

Figure 12: Basins of coexisting (a) 4-cycle $\mathbf{1}^2\mathbf{2}^2$ and two symmetric to each other 17-cycles, $\mathbf{1}^2(\mathbf{3}^1\mathbf{1}^2)^4\mathbf{2}^3$ and $\mathbf{2}^2(\mathbf{4}^1\mathbf{2}^2)^4\mathbf{1}^3$; (b) 4- and 6-cycles, $\mathbf{1}^2\mathbf{2}^2$ and $\mathbf{1}^3\mathbf{2}^3$, and two symmetric to each other 23-cycles, $\mathbf{1}^2(\mathbf{3}^1\mathbf{1}^2)^3\mathbf{2}^3\mathbf{1}^2(\mathbf{3}^1\mathbf{1}^2)\mathbf{1}^1\mathbf{2}^3$ and $\mathbf{2}^2(\mathbf{4}^1\mathbf{2}^2)^3\mathbf{1}^3\mathbf{2}^2(\mathbf{4}^1\mathbf{2}^2)\mathbf{2}^1\mathbf{1}^3$; the inset shows the indicated rectangle enlarged. Here (a) $(m_x, m_y) = (\tan(1.0725), \tan(0.451))$; (b) $(m_x, m_y) = (\tan(1.08), \tan(0.455))$. See the parameter points marked by white and yellow circles, respectively, in Fig.10a.

clarify why the overall bifurcation structure of region R_{IV} is quite complicated. Even if the boundaries of the periodicity regions forming each particular structure can be obtained analytically, in general it is a challenging task to list all the possible structures and to give the conditions of their existence depending on δ_x and δ_y.

7 Conclusion

In this paper we study a 2D piecewise linear discontinuous map depending on four parameters, which is a generalization of the map investigated in [7]. The considered map is associated with a more generic discrete-time version of the fashion cycle model proposed by Matsuyama in [12]. We show that in the parameter space of the map there is a standard period adding structure related to border attractors, there are also numerous incrementing structures with distinctive properties, as well as novel bifurcation structures of mixed type caused by an interplay between period adding and period incrementing bifurcation structures. We propose an explanation of the mechanism of creation of these mixed structures, however, their complete description is still missing. We leave it for future investigation, as well as the case $\delta_x < \delta_y$, not considered in the present paper.

Acknowledgements I. Sushko thanks the University of Urbino for the hospitality experienced during her stay there as a Visiting Professor. K. Matsuyama is also grateful to the University of Urbino for the hospitality during his visit.

References

[1] Avrutin V, Gardini L, Sushko I, Tramontana F. Continuous and discontinuous piecewise-smooth one-dimensional maps: invariant sets and bifurcation structures. World Scientific; 2019 (to appear).

[2] Avrutin V, Schanz M, Gardini L. Calculation of bifurcation curves by map replacement. Int. J. Bif. Chaos 2010; 20:3105-3135.

[3] Avrutin V, Sushko I. A gallery of bifurcation scenarios in piecewise smooth 1D maps. In: Bischi GI, Chiarella C, Sushko I, editors. Global analysis of dynamic models for economics, finance and social sciences. Springer; 2013.

[4] di Bernardo M, Budd CJ, Champneys AR, Kowalczyk P. Piecewise-smooth dynamical systems: theory and applications, applied mathematical sciences, vol. 163. London: Springer-Verlag; 2008.

[5] Boyland PL. Bifurcations of circle maps: Arnold tongues, bistability and rotation intervals. Comm. Math. Phys. 1986; 106(3)**:**353-381.

[6] Gardini L, Avrutin V, Sushko I. Codimension-2 border collision bifurcations in one-dimensional discontinuous piecewise smooth maps. Int. J. Bif. Chaos 2014; 24(2):1450024 (30 pages).

[7] Gardini L, Sushko I, Matsuyama K. Bifurcation structure in a 2D discontinuous map: explanation of fashion cycles. CHAOS 2018; 28:055917.

[8] Homburg AJ. Global aspects of homoclinic bifurcations of vector fields. Berlin: Springer-Verlag; 1996.

[9] Keener JP. Chaotic behavior in piecewise continuous difference equations. Trans. Am. Math. Soc. 1980; 261:589–604.

[10] Leonov NN. Map of the line onto itself. Radiofisika 1959; 3:942–956.

[11] Lyubimov DV, Pikovsky AS, Zaks MA. Universal scenarios of transitions to chaos via homoclinic bifurcations. Math. Phys. Rev. 1989; 8 Harwood Academic, London.

[12] Matsuyama K. Custom versus Fashion: Path-dependence and Limit Cycles in a Random Matching Game. Discussion paper N 1030, 1992, Dept of Economics, Northwestern University.

[13] Mira C. Embedding of a Dim1 Piecewise Continuous and Linear Leonov Map into a Dim2 Invertible Map. In: Bischi GI, Chiarella C, Sushko I, editors. Global analysis of dynamic models for economics, finance and social sciences. Springer; 2013.

[14] Nusse HE, Yorke JA. Border-collision bifurcations including period two to period three for piecewise smooth systems. Physica D 1992; 57:39–57.

[15] Tramontana F, Sushko I, Avrutin V. Period adding structure in a 2D discontinuous model of economic growth. Appl. Math. and Comput.2015; 253:262273.

[16] Zhusubaliyev ZT, Mosekilde E. Bifurcations and chaos in piecewise-smooth dynamical systems. Nonlinear Science A Vol. 44. World Scientific; 2003.